Exp Brain Res (1992) 88:131–139

Experimental Brain Research

Involvement of local ischemia in endothelin-1 induced lesions of the neostriatum of the anaesthetized rat

K. Fuxe[1], N. Kurosawa[2], A. Cintra[1], Å. Hallström[2], M. Goiny[2], L. Rosén[1], L.F. Agnati[2] and U. Ungerstedt[2]

[1] Department of Histology and Neurobiology, and [2] Department of Pharmacology, Karolinska Institutet, Box 60400, S–10401 Stockholm, Sweden
[3] Department of Human Physiology, University of Modena, Modena, Italy

Received May 7, 1991 / Accepted July 26, 1991

Summary. The present study examines the possibility that lesions induced by intrastriatal injections of endothelin-1 (ET–1, 0.43 nmol/0.5 μl) are ischemic in nature due to a vasoconstriction of the cerebral microvessels. In time course and dose-response experiments with ET–1 and in comparisons with ET–3, the volume of the lesions has been determined based mainly on the disappearance of striatal nerve cells, using a computer assisted morphometrical analysis. The blood flow in the neostriatum close to the site of injection of ET–1 was determined acutely by Laser-Doppler flowmetry. The acute metabolic effects of ET–1 were also studied on striatal superfusate levels of lactate, pyruvate, dopamine and its metabolites DOPAC (3,4-dihydroxyphenylacetic acid) and homovanilic acid (HVA) using an instrastriatal microdialysis probe. Dose related striatal lesions were observed with ET–1 (0.043–0.43 nmol) with a peak lesion volume after 24–48 h and the possible existence of a penumbra area. ET–3 showed a reduced potency to produce striatal lesions compared to ET–1. The lesions induced by ET–1 were prevented by coinjection with dihydralazine, a vasodilator drug. Acutely ET–1 (0.43 nmol/0.5 μl) produced a prolonged reduction of the cerebral blood flow down to 40% of control values and temporary increases of striatal lactate and DA efflux, the latter change being very marked. Also a significant reduction of DOPAC and HVA was observed. These neurochemical changes were all prevented by treatment with dihydralazine. These results indicate that ET–1 injected in the neostriatum may produce lesions by causing local ischemia, related to its vasoconstrictor activity and possibly also to an activation of ET–1 receptors in the astroglial-endothelial complex. Based on the present results it seems possible that ET–1 may participate in the multifactorial pathogenesis of cerebral ischemia.

Key words: Endothelin – Ischemia – Striatum – Microdialysis – Cerebral blood flow – Rat

Offprint requests to: K. Fuxe

Introduction

Endothelin-1 (ET–1) is a recently isolated endothelin-derived 21-amino acid residue which possesses a powerful and long-lasting vasoconstrictor action (Yanagisawa et al. 1988). Besides ET–1 immunoreactivity (IR), ET–3 like IR has been demonstrated in porcine spinal cord and brain (Inoue et al. 1989; Shinmi et al. 1989; Matsumoto et al. 1989; Fuxe et al. 1991a). ET–3 is also a bicyclic 21 amino acid peptide having a 71% sequence homology with ET–1 (Yanagisawa et al. 1988; Inoue et al. 1989). Immunocytochemical evidence exists on both a glial and neuronal location of ET-like IR, especially in activated astroglia (Cintra et al. 1989; Fuxe et al. 1989b, 1991a; MacCumber et al. 1990; Giaid et al. 1989; Yoshishawa et al. 1990). Also ET–1 mRNA has been found to be expressed in porcine and human brain (Nunez et al. 1990). Recently, it has also been demonstrated tht ET–3-like IR exists within somatostatin (SS) and choline acetyltransferase (ChAT) IR nerve cells of the neostriatum of the rat (Fuxe et al. 1991a), suggesting a neuronal role of ET–3-like peptides in the CNS (see also Matsumoto et al. 1989; Shinmi et al. 1989). Finally, evidence exists for the presence of ^{125}I–ET–1 and ^{125}I–ET–3 binding sites within the CNS, the latter having a regional distribution (Fuxe et al. 1989c; Jones et al. 1989; MacCumber et al. 1990; Koseki et al. 1989; Marsault et al. 1989; Vigne et al. 1990). As shown by Marsault et al. (1989), the ET receptor located on the astrocytes possesses also a high affinity for ET–3, which is not true for the ET receptor located on the brain capillary ET cells (Vigne et al. 1990).

We have recently demonstrated that centrally administrated ET–1 induces lesions in the brain of the male rat by producing a disappearance of striatal nerve cells (Fuxe et al. 1989a, 1991b). It was suggested that this may represent a new model of local brain ischemia with a high physiopathological relevance. In line with this view it has been found that cerebral microvessel endothelial cells can

produce ET (Yoshimoto et al. 1990) and ET-1 can produce vasoconstriction of cerebral arteries from the adventitial side (Shigeno et al. 1989). Also it has been found that ET can trigger brain damage under hypoglycemia (Kataoka et al. 1989).

To test the hypothesis that ET-1 induces a focal ischemia we have in the present paper analyzed the effects of an intrastriatal injection of ET-1 in the absence or presence of the potent vasodilator drug, dihydralazine, on striatal blood flow, and extracellular striatal levels of lactate, pyruvate, and dopamine (DA) and its metabolites DOPAC (3,4-dihydroxyphenylacetic acid) and homovanilic acid (HVA), in halothane anaesthetized rats. For comparison the effects of intrastriatal injections of ET-3 have been analysed which may not as effectively stimulate the ET-1 receptors of the cerebral microvessels. Furthermore, a computer-assisted analysis of the neostriatal lesion, in the absence or presence of dihydralazine, has been carried out on suitable histological preparations.

Material and methods

Male Sprague-Dawle rats ($n=11$) were anaesthetized with halothane (1.0–1.3% in air). The anaesthetic concentration was controlled by the use of a vaporizer. Respiration was maintained through a trachea cannula connected to an artificial respirator. Pa CO_2 levels was set at 30–40 mm Hg and pa O_2 levels at 100–120 mmHg (normoxemia). Rectal temperature was maintained at 37.5° C ± 0.2° C by means of thermoregulatory heating pad (CMA/150, Carnegie Medicin, Sweden). Blood pressure was monitored continuously from the left femoral artery and ranged in different rats between 90 and 110 mmHg.

The rat's head was fixed in a stereotaxic frame (David Kopf), and the animal was placed in a prone position. An approximately rectangularshaped piece of skull bone 3–4 mm in length (anterocaudal) and 4–5 mm in width (medial-lateral) was drilled out on one side. A small needle (32 gauge) for injection of drugs was attached to a coaxial microdialysis probe covered by a dialyzing membrane of 3.0 mm in length and 0.5 mm in diameter (CMA/10, Carnegie Medicin). The microdialysis probe was implanted into the caudate-putamen to a depth of 6.2 mm (V–6.2 mm) from the cortical dura surface at 0.9 mm anterior (A + 0.9 mm) and 3.5 mm lateral (L + 3.5 mm) to the Bregma, together with the injection needle (A + 0.9 mm; L + 3.0 mm; V–4.7 mm), according to the rat brain stereotaxic coordinates outlined in the atlas of Paxinos and Watson (1982). The microdialysis probe was perfused at a rate of 2 µl/min with Ringer through the inlet using a microinjection pump (CMA/100, Carnegie Medicin). About 1 h after the insertion of the probe into the caudate-putamen and the initiation of the perfusion, the dialysates were collected every 20 min into a sample tube containing 5 µl of 0.01 N HCl.

The microdialysis samples (40 µl) were divided into two aliquots, one (10 µl) was for analysis of lactate and pyruvate, the other (30 µl) was for that of DA, DOPAC and HVA. The in vitro recovery rates of lactate, pyruvate, DA, DOPAC and HVA by the microdialysis method were 20–25%. Both aliquots were injected, without any pretreatment, into high-performance liquid chromatography (HPLC) systems. The two HPLC methods have been described elsewhere (Hallström et al. 1989; Hurd and Ungerstedt 1989).

Briefly, lactate and pyruvate were separated on a resin-based column (precolumn polypore H (PPH–GU) 30 × 4.6 mm I.D.) and an analytical column 220 × 4.6 mm 10 µm polypore H (PPH–224, Brownlee Laboratories, USA) using 2.5 mM sulphuric acid with a flow rate of 0.3 ml/min. Lactate and pyruvate were detected by an ultraviolet detector at 214 nm (UV–8, Bioanalytical Systems, USA). DA and its metabolites (DOPAC and HVA) were separated on a reversed phase column (5 µm) (250 × 2.0 mm I.D., Spherisorb ODS I, Knauer, FRG) using 0.13 M NaH_2PO_4 buffer (pH 4.35) containing 0.89 mM EDTA, 1.3 mM S-octylsulfate and 14% methanol, with a flow rate of 0.3 ml/min. Electrical detection was performed by means of a glassy carbon working electrode (LC–4A, Bioanalytical Systems, USA) set at +0.7 V. The minimum detection limits (signal-to-noise ratio of 2) for DA was 0.01 pmol.

Simultaneously, a probe (0.45 mm in diameter) belonging to a laser Doppler flowmeter (PF3, Perimed, Sweden) was inserted into the caudate putamen with a lateral inclination of 15° to a depth of 5 mm from the cortical surface at 0.9 mm anterior and 1.3 mm lateral to the Bregma, with its tip close to that of microdialysis probe, as shown in Fig. 1. The flux signal from the Laser velocymetry (LDF) was averaged with a 5 s time constant and the signal was recorded continuously on a pen recorder. The post-mortem signal was considered as baseline (0%) and subtracted from the LDF values. For details, see Skarphedinsson et al. (1988).

After taking three control microdialysis samples, i.e. after measuring blood flow for about 120 min, ET-1 (0.43 nmol) (human, porcine, Peninsula Lab., USA), ET-1 plus dihydralazine (53 nmol) (Ciba-Geigy) or mock CSF were administered through a small needle which had been implanted together with the microdialysis probe. Dihydralazine produces a vasodilatation by a direct action on the smooth muscle cells (Nickerson 1974). These drug solutions (0.5 µl) were administered over a 20 min period at a rate of 25 nl/min. ET-1 was dissolved in a mock cerebrospinal fluid (CSF) solution (ET-1 alone) or in dihydralazine solution (ET-1 plus dihydralazine). In control experiments dihydralazine (53 nmol) alone was administered as described above.

The values of blood flow and blood pressure were measured every 20 min after the onset of the drug administration and expressed as percentages of the respective value found 1 min before the drug administration. The magnitudes of the responses of lactate, pyruvate, DA, DOPAC and HVA to the administration of drugs were expressed as percentages of the concentration in the pre-injection fraction. The statistical significance was evaluated by analysis of variance and Duncan's test.

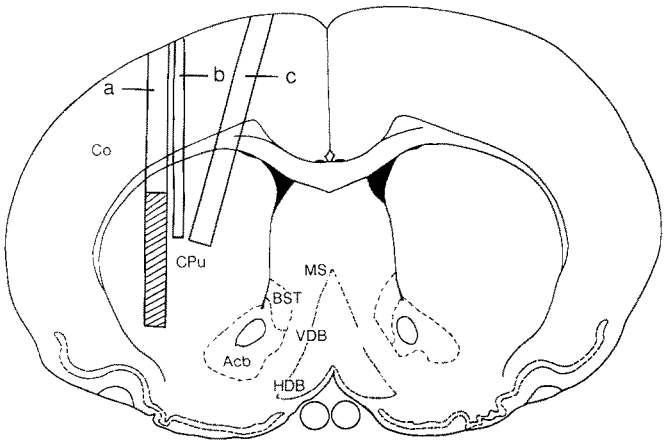

Fig. 1. Schematic illustration of the experimental procedure to record simutaneously striatal blood flow using Laser Doppler flowmetry and HPLC measurements of DA, DOPAC, HVA and lactate extracellular levels via microdialysis after injection of ET-1 in the halothane anaesthetized rat. CPu = nucleus caudatus-putamen; Co = cortex cerebri; BST = bed nucleus of the striae terminalis; MS = medial septal nucleus; Acb = nucleus accumbens; VDB and HDB = vertical and horizontal limb of the diagonal band

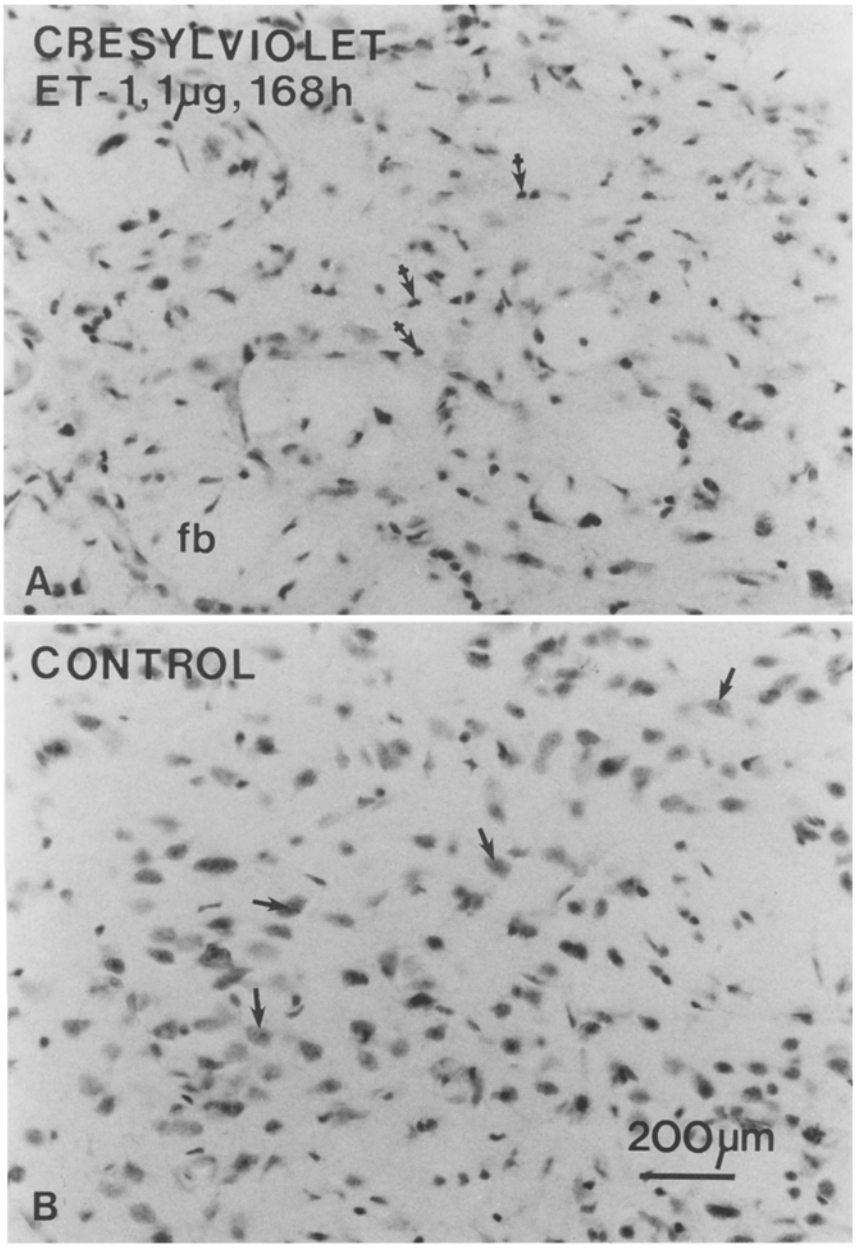

Fig. 2a, b. Cresylviolet stained coronal sections of the rat striatum 168 hr after local injection of 1 µg ET–1 (**a**). The medium sized striatal neurons have disappeared. For comparison see arrows in (**b**) which represents a section taken from a control animal. Small pycnotic nuclei (arrows with bar in **a**) are abundant probably belonging to the microglia. Bregma level 1.2 mm. fb striatal fiber bundle

Histological analysis

In separate experiments the ET–1-induced neostriatal lesions were taken to histological analysis involving transcardiac perfusion with 4% ice-cold paraformaldehyde in 0.1 M phosphate buffer under sodium pentobarbital anaesthesia (40 mg/kg, i.p.) followed by Nissl-staining (cresylviolet) and astroglia staining using GFAP immunocytochemistry (Fuxe et al. 1989a). The volume of the lesion was determined by means of a computer-assisted morphometrical analysis using the IBAS image analysis system (see Agnati et al. 1988; Zoli et al. 1990). Thus, serial cryostate sections (20 µm thick) of the neostriatum were made and the lesion area determined every 100 µm based on the disappearance of Nissl staining due to the chromatolysis (3 h time interval) or mainly due to the disappearance of nerve cells (later time intervals; Fig. 2) as previously demonstrated (Fuxe et al. 1989a). In the outer zone of the lesion some large striatal nerve cells were found, probably representing cholinergic cells, which may be more resistent to the insult (Fuxe et al. 1991b). In view of the fact that the lesion area is to a certain degree dependent on the phenomenon of chromatolysis a possible reduction with time (see results) of the lesion may be related to the recovery of the chromatolytic phenomenon in the medium sized striatal neurons. Thus, a penumbra area exists with affected nerve cells which are destined to survive or to undergo cell death. The lesion area could also be determined by the disappearance of GFAP IR in the affected area and strong GFAP IR was present in the border zone of the lesion and largely surrounded the lesioned area (Fig. 3) (Fuxe et al. 1989a; Fuxe et al. 1991b). Previous work (Fuxe et al. 1989a, 1991b) has also demonstrated that the ET–1 induced striatal lesions are associated with damage to the white fiber bundles of the neostriatum with degenerative changes in the oligodendroglia. Two types of experiments have been performed: a time-course experiment involving an analysis of the lesion at 3, 24, 48 and 144 h following the injection of 0.43 nmol (in 0.5 µl mock CSF) of ET–1 and a dose-response experiment evaluated at the 144 h time interval with ET–1 and ET–3 (0.043, 0.129 and 0.43 nmol in 0.5 µl in mock CSF). Finally, an experiment was performed in which it was evaluated if the vasodilator drug dihydralazine (53 nmol) given together

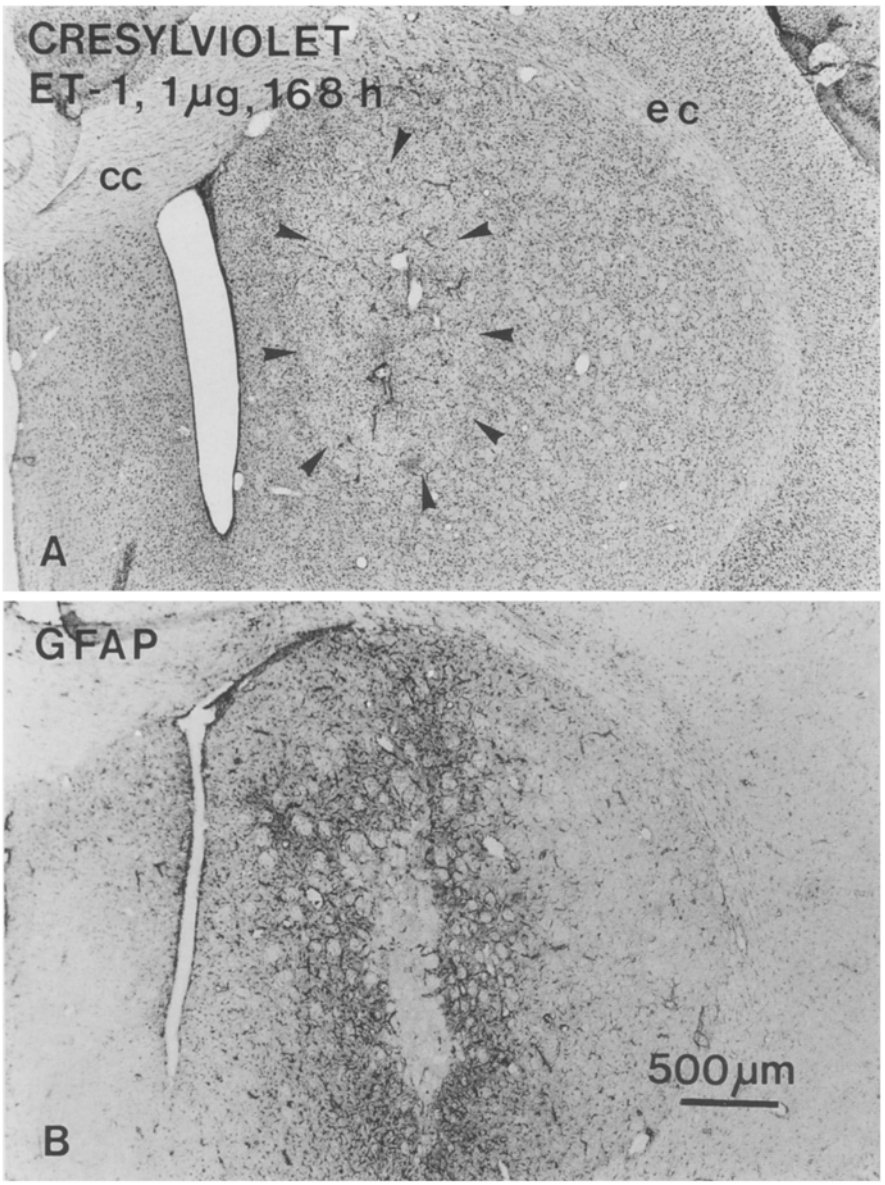

Fig. 3. GFAP IR of the neostriatum is demonstrated (Fig. 2B) in coronal cryostate (14 µm) sections at Bregma level +1.2 mm 168 h after the ET–1 injection (0.43 nmol/0.5 µl). The absence of nerve cells in the injected area is outlined in A (cresylviolet). The lesioned area is surrounded by a zone of strong GFAP IR, which is also present in the outer part of the lesioned area. A rabbit anti-cow GFAP antiserum (Dakopatts; 1:1000) was employed and the detection of the GFAP IR was made by the avidin-biotin-peroxidase technique using 3,3'-diaminobenzidine as the chromophore. cc = corpus callosum; ec = external commissure

with ET–1 could counteract the ET–1-induced neostriatal lesion (0.43 nmol) as evaluated at the 144 h time interval. ET–1 and ET–3 were always injected in a volume of 0.5 µl mock CSF using the same coordinates as described above with an infusion period of 20 min (see above). The statistical analysis was performed by means of the Mann-Witney U test or the test treatment versus control (Hollander and Wolfe 1973).

Results

Histological studies

Histological analysis of the ET–1-induced neostriatal lesion. The time-course of the ET–1 (0.43 nmol/0.5 µl) induced neostriatal lesion was studied at the 3 h, 24 h, 48 h and 168 h time interval. At the 24–48 h time interval ET–1 produced the maximal lesion with a mean volume in the order of 6 mm^3 (Fig. 4). The shape of the lesion was somewhat assymetric with a larger extension in the caudal direction (appr. 1.5 mm) as illustrated at the 168 h time interval (Fig. 5). At the earliest time interval (3 h) nerve cells were still present in the injected area but they were shrunk and exhibited chromatolysis. The affected volume was similar to the volume of lesion based on disappearance of nerve cells (Fig. 2) found at the 24 and 48 h time intervals. At the 168 h time interval the ET–1-induced lesion had become reduced to a mean volume of 4.0 mm^3 as defined above by Nissl staining (Fig. 3) indicating that a penumbra area developed upon ET–1 injections in the neostriatum (see material section). Infusion of mock CSF alone produced only a small mechanical lesion, which amounted to a volume of 0.2 mm^3 at the 168 h time interval, which was approximately 5% of the ET–1-induced lesion (Fig. 5).

Dose-response experiments. As seen in Fig. 6, ET–1 appeared to be highly effective in producing a striatal lesion already at a dose of 0.1 µg (0.043 nmol)/0.5 µl while ET–3 was only weakly effective in a dose of 0.1 or 0.3 µg/

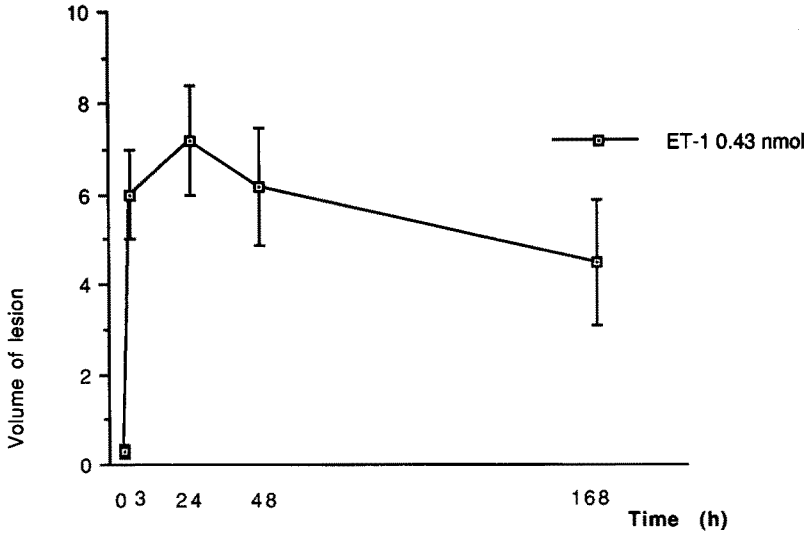

Fig. 4. Morphometrical analysis of the time-course of the development of the lesion volume (in mm^3) after an ET–1 injection (0.43 nmol/0.5 µl) into the neostriatum based on Nissl stainings allowing the determination of the lesion area at each rostrocaudal level. A chromatolysis of the nerve cells was evident already at the 3 h time interval, but the nerve cells were still visible at this time interval. Therefore, after 3 h the affected area mainly represents the chromatolytic area. The formula for the calculation of the volume (in mm^3) is: $\Sigma_{2\ n}[(A_i + A_{i-n}):2] \times d$ A_i = area of lesion; n = number of sections. The interlevel distance along the rostrocaudal axis is equal to d. Means ± SEM are shown out of 3–4 rats

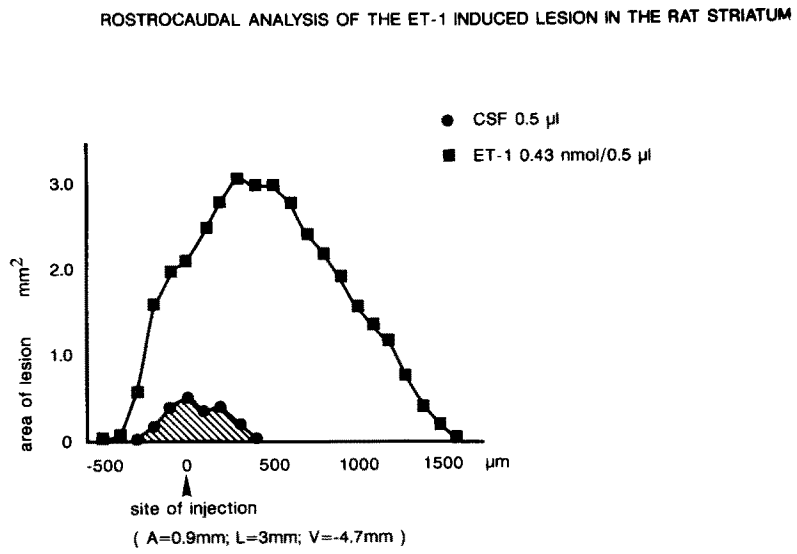

Fig. 5. Morphometrical analysis of the ET–1 induced neostriatal lesion as evaluated at the 168 h time interval using the IBAS image analysis system (Agnati et al. 1988). The mean values of 4 rats are shown at each level analyzed. The measurements of the lesion area was made by outlining the area of nerve cell disappearance and microglia infiltration as seen in Nissl stainings. The hatched area represents the lesion area produced by a mock CSF injection (0.5 µl). The lesion extends preferentially in the caudal direction probably due to the fact that the cannula opened in the caudal direction

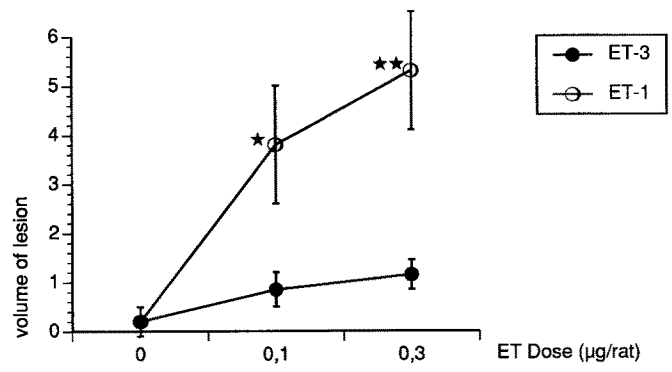

Fig. 6. Morphometric analysis of the ET–1 and ET–3 induced neostriatal lesions using two doses, 0.01 µg and 0.3 µg (0.043 and 0.129 nmol/0.5 µl) at the 168 h time interval. The mean volume (in mm^3) of the lesion is given as means ± SEM out of 3–4 rats. For details, see text to Fig. 3. Statistical analysis according to the test treatment vs control (non-parametrical procedures). * = $P < 0.05$; ** = $P < 0.01$

0.5 µl. The lesion volume after ET–3 was in the order of 1 mm^3.

Effects of dihydralazine on the ET–1-induced neostriatal lesion. As seen in Fig. 7 dihydralazine (53 nmol/0.5 µl) was able to significantly reduce the ET–1-induced neostriatal lesion at the site of ET–1 injection, where the maximal lesion was observed, as evaluated in Nissl stainings and in studies on GFAP IR at the 168 h time interval. ET–1 and dihydralazine were injected together in the same 0.5 µl solution. The maximal lesion area produced by mock CSF alone was in the order of 10% of the respective striatal area.

Functional and neurochemical studies

Effects of intraneostriatal injections of ET–1 on striatal blood flow. As evaluated by laser-Doppler flowmetry

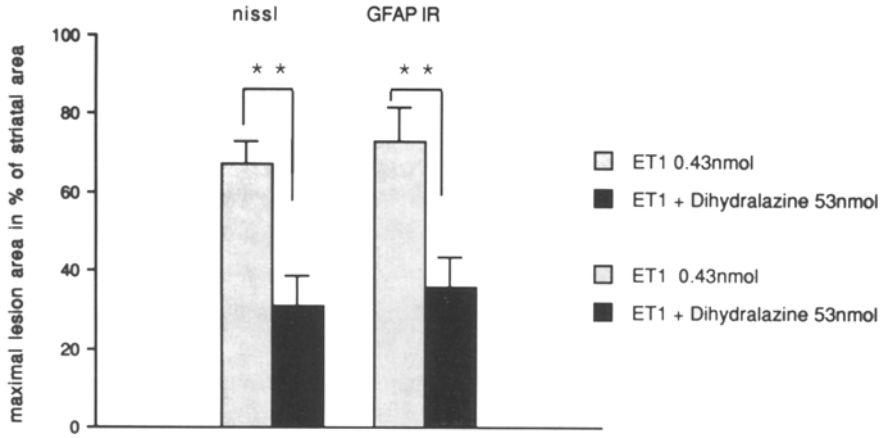

Fig. 7. Effects of dihydralazine and on the ET–1 induced lesion in the neostriatum seen after local injection of ET–1. The lesion was evaluated at the level where the lesion was maximal as revealed by Nissl staining and GFAP IR. Dihydralazine was infused together with ET–1. ** = $P < 0.01$, Mann-Whitney U-test

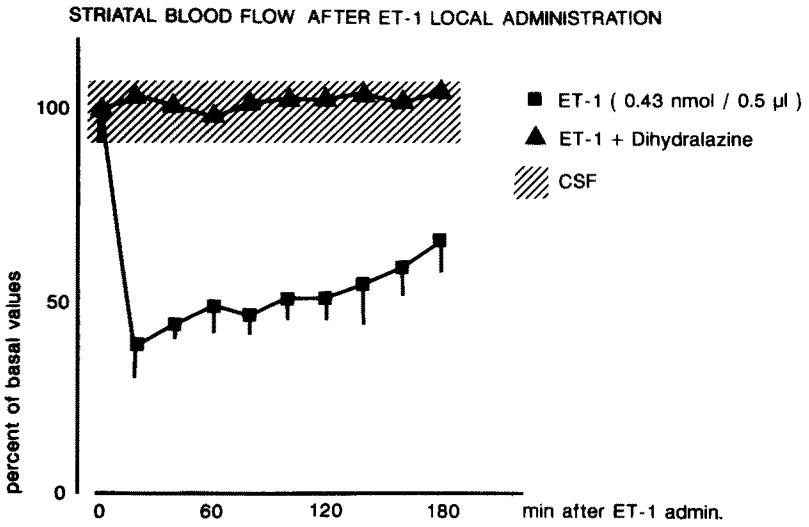

Fig. 8. Effects of a neostriatal injection of ET–1 in the absence or presence of the vasodilator dihydralazine (53 nmol/0.5 µl) on striatal blood flow using Laser Doppler flowmetry in the halothane anaesthetized rat. Means ± SEM (100% = 147 ± 29 LDF units) are shown out of 3–4 rats in the ET–1 alone group. A similar variability was found in the other two groups. The striatal blood flow is given in arbitrary units. The hatched area gives the overall s.e.m. of the CSF alone group during the 3 h period. Duncan's test after one way analysis of variance. The ET–1 alone group is significantly ($P < 0.01$) different from the other two experimental groups at all time intervals studied

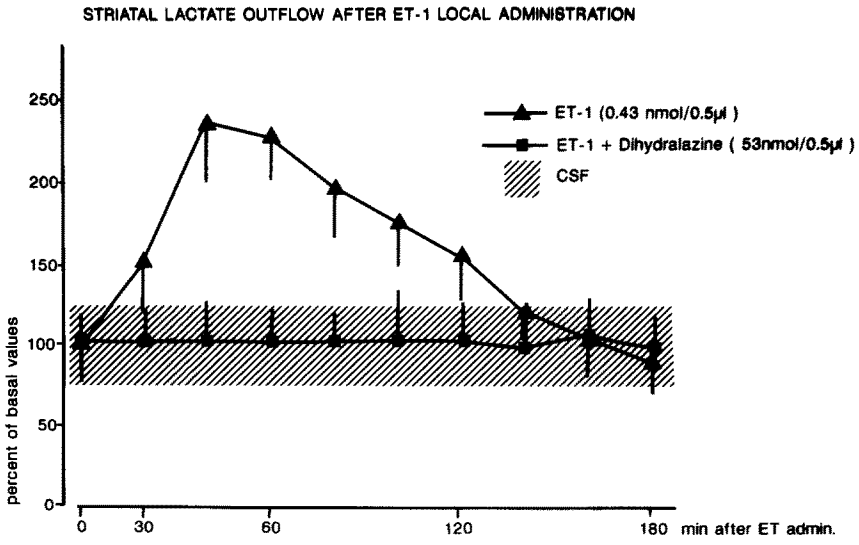

Fig. 9. Effects of a neostriatal injection of ET–1 in the absence or presence of dihydralazine (53 nmol/0.5 µl) on striatal lactate outflow in the halothane anaesthetized rats. Means ± SEM (100% = 232 ± 24 µM) out of 3–4 rats. The *hatched area* gives the overall s.e.m. in the CSF alone group over the 3 h period. Duncan's test after one way analysis of variance. The ET–1 group is significantly different from the other two groups from the 20 to the 100 min time interval. At the 20 and 100 min time interval the significance is $P < 0.05$; at the 40, 60 and 80 min time intervals it is $P < 0.01$

ET–1 in a dose of 0.43 nmol produced about a 60% reduction in striatal blood flow which was observed within 20 min and largely maintained throughout the 3 h observation period with only a small gradual return (40% reduction at the end of the 3 h period) (Fig. 8). The mock CSF alone did not alter striatal blood flow. Furthermore, dihydralazine given as described above counteracted the ET–1-induced reduction of striatal blood flow (Duncan's test).

Studies on the effects of neostriatal injections of ET–1 on striatal lactate outflow. By means of microdialysis it was

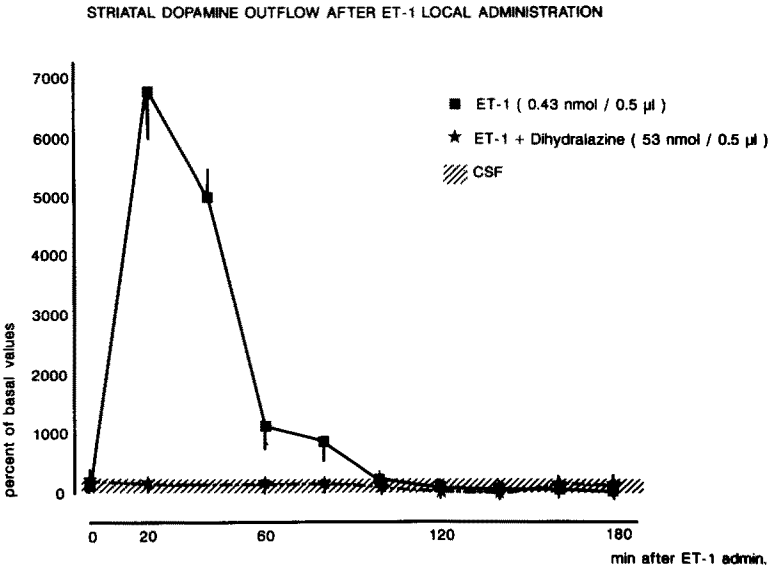

Fig. 10. Effects of a neostriatal injection of ET–1 in the absence or presence of dihydralazine (53 nmol/0.5 µl) on striatal dopamine outflow in the halothane anaesthetized rat. Means ± SEM (100% = 4.2 ± 1.3 nM) are shown out of 3–4 rats. The hatched area represents the overall s.e.m. in the CSF group over the 3 h period. Duncan's test after one way analysis of variance. The ET–1 alone group is significantly different ($P < 0.01$) from the other two groups from the 20 to the 60 min time interval

shown that ET–1 (0.43 nmol/0.5 µl) significantly increased lactate levels in striatal superfusates with a peak increase of about 230% at the 40 min time interval (Fig. 9). From the 40 min time interval the increase in striatal lactate outflow gradually declined and control levels were restored at the 160 min time interval. The dihydralazine treatment, as described above, was found to completely counteract the increase in striatal lactate outflow (Fig. 9).

Effects of neostriatal injection of ET–1 on striatal pyruvate outflow. ET–1 (0.43 nmol/0.5 µl) did not significantly ($P = 0.1$) alter the striatal pyruvate outflow but a trend for a small reduction was observed throughout the 3 h observation period [peak action = 75 ± 25% of basal value (8.8 ± 1.2 µM)]. This trend for a reduction of striatal pyruvate outflow was no longer observed following combined treatment with ET–1 and dihydralazine.

Effects of neostriatal ET injection on striatal DA outflow. As seen in Fig. 10, ET–1 (0.43 nmol/0.5 µl) produced a huge (larger than 6000%) increase in striatal DA outflow which was maximal already at the 20 min time interval after which it declined rapidly and reached control levels at the 2 h time interval. This increase of striatal DA outflow was completely counteracted by the simultaneous infusion of dihydralazine. During the period of increased striatal DA there was a significant reduction in the order of 30–40% of the superfusate levels of DOPAC [peak action = 61% ± 15% of basal value (437 ± 94 nM); $P < 0.001$] and HVA [peak action = 70 ± 7% of basal value (304 ± 87 nM); $P < 0.01$]. Also the effects on the outflow of DA metabolites were counteracted by the simultaneous treatment with dihydralazine.

Discussion

In the present paper indications have been obtained that ET–1-induced local striatal lesions may be produced via a local ischemia. Firstly, the morphological evidence indicates that the powerful vasodilator dihydralazine can significantly counteract the lesion induced in the neostriatum by local injection of ET–1. Secondly, evidence is presented by means of laser Doppler flowmetry that ET–1 locally injected in the neostriatum can produce a prolonged and marked reduction of striatal blood flow, an action of ET–1 which also is counteracted by simultaneous treatment with dihydralazine. As previously observed in animal models of transient forebrain ischemia (see Zini et al. 1990) striatal lactate and DA outflow were also substantially increased upon injection with ET–1 into the neostriatum and these actions were counteracted by dihydralazine. Based on this experimental evidence the following hypothesis is given as to the mechanism underlying the ET–1-induced lesion of the neostriatum following a local infusion.

Reduction of the cerebral blood flow observed in the neostriatum upon local ET–1 infusion (into the neostriatum) is probably caused by the powerful vasoconstrictor activity of ET–1 (Shigeno et al. 1989). It has also been demonstrated by Shigeno et al. (1989) that the vasoconstriction produced by ET–1 of cerebral arteries involves an action from the adventitial side. Although a prolonged vasoconstriction was observed during the 3 hour observation period it must be emphasized that there was a gradual increase of striatal blood flow from 40 to 60% of control value from the 20 min to the 180 min time interval. It seems possible that this increase in striatal blood flow, although relatively small, is sufficient to explain the normalization of striatal lactate and DA outflow at the end of the 3 h observation period. It is possible that a small increase of blood flow may in fact increase survival of nerve cells by bringing the blood flow over a certain threshold level necessary for survival. In spite of the restoration of striatal metabolism during the 3 h time period following ET–1 perfusion the prolonged vasoconstriction appears to be of importance for the development of the ET–1-induced lesion, since dihydralazine can markedly counteract the development of the lesion, which is probably related to its ability to counteract the

reduction of striatal blood flow induced by ET–1. Also at the end of the 3 h period the nerve cells in the injected area are shrunk and show chromatolysis. Thus, it seems possible that the final development of the ET–1 striatal lesion is related to a post-ischemic hypoperfusion of the neostriatum, at least in part triggered by the ET–1 induced vasoconstriction. Direct effects of injected ET–1 on the endothelial cells may also contribute (see last part of discussion). The above hypothesis may, however, be questioned, since a fall of cerebral blood flow down to 15% of the normal has generally been considered necessary to produce cerebral ischemia in the middle cerebral artery occlusion (Bolander et al. 1989) and only a reduction down to 40% of control was observed using Laser-Doppler flowmetry in the present experiments. Such a model of regional and permanent cerebral ischemia may be the most suitable to compare with the methodology used in this study. However, it must be considered that the Laser Doppler probe was located some distance away from the cannula used to inject ET–1 and thus, other striatal areas closer to the lesion may well have reached a value of reduction of cerebral blood flow leading to ischemia. This possibility, which is supported by the reversal obtained with dihydralazine, will be evaluated in future work using quantitative iodoantipyrine autoradiography. It should, however, be considered that ET–1 induced release of striatal DA could have contributed to the development of the striatal lesion, since it was partly counteracted by a D1 receptor antagonist (Fuxe et al. 1991b). Nevertheless, lesions induced by locally injected ET–1 develop also in other brain areas, containing only few DA nerve terminals such as the hippocampal formation (Fuxe et al. 1991b). Finally, calcium antagonists of the dihydropyridine family also partly antagonized the development of the ET–1 lesion in the neostriatum (Fuxe et al. 1991b), which may be related not only to their neuroprotective activity (see review by Siesjö and Bengtsson, 1988), but also probably to a reduction of the ET–1 induced vasoconstriction, which may involve Ca^{++} ions as a second messenger (Symon 1989).

We now propose that the post-ischemic hypoperfusion may be related to the activation of ET mechanisms within the astroglia (see Cintra et al. 1989; Fuxe et al. 1989; MacCumber et al. 1989, 1990) and within the cerebral microvessel endothelial cells (Yoshimoto et al. 1990). Thus, not only can astrocytes and cerebral capillary endothelial cells produce ET upon activation by e.g. ischemia but they also possess ET–1 receptors (Cintra et al. 1989; Marsault et al. 1990; Lin et al. 1990) leading to mitogenesis and increases of free calcium (Supattapone et al. 1989). Furthermore, only ET–1 receptors are located on the endothelial cells (Marsault et al. 1990) and it is of interest to note that ET–3 was subtantially less potent than ET–1 in producing lesions in neostriatum upon local infusion. It has been demonstrated that ET–1 can activate phosphatidyl inositol hydrolysis and increase DNA synthesis in cerebral capillary endothelial cells (Lin et al. 1990). These events probably also lead to a mobilization of intracellular calcium due to formation of inositoltriphosphate, which may lead to an activation of the contractile proteins within the endothelial cells, contributing to the reduction of blood flow. Evidence in fact exists that ET-like peptides are formed within astroglia surrounding cerebral microvessels in ischemic areas (Fuxe et al. 1991b). ET peptides released from astroglia surrounding capillary vessels as well as injected ET–1 may thus cause activation of the ET–1 receptors located on the endothelial cells leading to a marked reduction of local cerebral blood flow (see above). It should be pointed out that the mitogenic response also can contribute to the mantained reduction. In agreement, ET–3 locally injected into the neostriatum is much less powerful than ET–1 in producing neostriatal lesions. Thus, the present and previous work (Fuxe et al. 1989a, b, 1991b; Cintra et al. 1989) may implicate local ET–1 mechanisms in the astroglial-endothelial complex as one of the mechanisms underlying the development of post-ischemic hypoperfusion and transient ischemic attacks in man.

In conclusion, the present paper gives morphological and neurochemical evidence that the ET–1-induced neostriatal lesions in the rat triggered by a prolonged initial vasoconstrictor action of ET–1, are produced via a local ischemia. It seems possible that such a lesions may represent a new in vivo model for local ischemia.

Acknowledgements. This work has been supported by a grant (04X–715) from the Swedish Medical Research Council and by a grant from Augusta and Petra Hedlunds Stiftelse.

References

Agnati LF, Fuxe K, Zoli M, Zini I, Härfstrand A, Toffano G, Goldstein M (1988) Morphometrical and microdensitometrical studies on phenylethanolamine-N-methyltransferase- and neuropeptide Y-immunoreactive neurons in the rostral medulla oblongata of the adult and old male rat. Neuroscience 26:461–478

Bolander HG, Persson L, Hillered L, d'Argy R, Ponten U, Olsson Y (1989) Regional cerebral blood flow and histopathologic changes after cerebral artery occlusion in rats. Stroke 20:930–937

Cintra A, Fuxe K, Änggård E, Tinner B, Staines W, Agnati LF (1989) Increased endothelin-like immunoreactivity in ibotenic acid-lesioned hippocampal formation of the rat brain. Acta Physiol Scand 137:557–558

Fuxe K, Cintra A, Andbjer B, Änggård E, Goldstein M, Agnati LF (1989a) Centrally administered endothelin-1 produces lesions in the brain of the male rat. Acta Physiol Scand 137:155–156

Fuxe K, Cintra A, Änggård E, Tinner B, Staines W, Agnati LF, Galton S, Vane JR (1989b) Increased formation of endothelin-like immunoreactivity in activated astroglia and its relation to ^{125}I-endothelin-1 binding sites in the rat brain. Neuroscience Abstr 15:126

Fuxe K, Änggård E, Lundgren K, Cintra A, Agnati LF, Galton S, Vane J (1989c) Localization of ^{125}I-endothelin-1 and ^{125}I-endothelin-3 binding sites in the rat brain. Acta Physiol Scand 137:563–564

Fuxe K, Tinner B, Staines W, Hemsén A, Hersh L, Lundberg JM (1991a) Demonstration and nature of endothelin-3 like immunoreactivity in somatostatin and choline acetyltransferase immunoreactive nerve cells of the neostriatum of the rat. Neurosci Lett 123:107–111

Fuxe K, Kurosawa M, Cintra A, Goiny M, Hallström Å, Rosén L, Ungerstedt U, Agnati LF (1991b) Endothelin-1 induced lesions in the brain as a new model of focal ischemia. In: Conn PM (ed)

Methods in Neurosciences, Vol. 7: Transplantations, Lesions and Surgical Techniques, Academic Press Inc, Orlando Florida (in press)

Giaid A, Gibson SJ, Ibrahim NBN, Legon S, Bloom SR, Yanagisawa M, Masaki T, Varndell IM, Polak JM (1989) Endothelin-1, an endothelin-derived peptide, is expressed in neurons of the human spinal cord and dorsal root ganglia. Proc Natl Acad Sci USA, 86:7634–7638

Hallström Å, Carlsson A, Hillered L, Ungerstedt U (1989) Simultaneous determination of lactate, pyruvate, and ascorbate in microdialysis samples from rat brain, blood, fat, and muscle using high-performance liquid chromatography. J Pharmacol Methods 22:113–124

Hollander M, Wolfe DA (1973) Nonparametrical statistical methods. Wiley, New York

Hurd YL, Ungerstedt U (1989) In vivo neurochemical profile of dopamine uptake inhibitors and releasers in rat caudate-putamen. Eur J Pharmacol 166:251–260

Inoue A, Yanagisawa M, Kimura S, Kasuya Y, Miyauchi T, Goto K, Masaki T (1989) The human endothelin family: three structurally and pharmacologicaly distinct isopeptides predicted by three separate genes. Proc Natl Acad Sci USA 86:2863–2867

Jones CR, Hiley CR, Pelton JT, Mohr M (1989) Autoradiographic visualization of the binding sites for ^{125}I-endothelin in rat and human brain. Neurosci Lett 97:276–279

Kataoka Y, Koizumi S, Kumakura K, Kurihara M, Niwa M, Ueki S (1989) Endothelin-triggered brain damage under hpoglycemia evidenced by real-time monitoring of dopamine release from rat striatal slices. Neurosci Lett 107:75–80

Koseki C, Imai M, Hirata Y, Yanagisawa M, Masaki T (1989) Autoradiographic distribution in rat tissues of binding sites for endothelin: a neuropeptide? Am J Physiol 256 (4 Pt 2):R858–866

Lin WW, Lee CY, Chuang DM (1990) Comparative studies of phosphoinositide hydrolysis induced by endothelin-related peptides in cultured cerebellar astroctes C6-glioma and cerebellar granular cells. Biochem Biophys Res Comm 168:512–519

MacCumber MW, Ross CA, Glaser BM, Snyder SH (1989) Endothelin: visualization of mRNAs by in situ hybridization provides evidence for local action. Proc Natl Acad Sci USA 86:7285–7289

MacCumber MW, Ross CA, Snyder SH (1990) Endothelin in brain: Receptors, mitogenesis, and biosynthesis in glial cells. Proc Natl Acad Sci USA 87:2359–2363

Marsault R, Vigne P, Breittmayer JP, Frelin (1989) Astrocytes are target cells for endothelins and sarafotoxin. J Neurochem 54:2142–2144

Matsumoto H, Suzuki N, Onda H, Fujino M (1989) Abudance of endothelin-3 in rat intestine, pituitary gland and brain. Biochem Biophys Res Comm 164:74–80

Nickerson M (1974) Antihypertensive agents and the drug therapy of hypertension. In: Goodman, LS, Gilman A (eds) The pharmacological basis of therapeutics 4 edn. The MacMillan Co, London, pp 728–734

Nunez DJ, Brown MJ, Davenport AP, Neylon CB, Schofield JP, Wyse RK (1990) Endothelin-1 mRNA is widely expressed in porcine and human tissues. J Clin Invest 85:1537–1541

Paxinos G, Watson C (1982) The rat brain in stereotaxic coordinates. Academic Press, New York

Shigeno T, Mima T, Takakura K, Yanagisawa M, Saito A, Goto K, Masaki T (1989) Endothelin-1 acts in cerebral arteries from the adventitial but not from the luminal side. J Cardiovasc Pharmacol 13 Suppl 5:S162–165

Siesjö BK, Bengtsson F (1988) Calcium, calcium antagonists, and ischemic celll death in the brain. In: Krieglstein J (ed) Pharmacology of the cerebral ischemia 1988. Wissenschaftliche Verlagsgesellschaft, Stuttgart, pp 23–28

Shinmi O, Kimura S, Sawamura T, Sugita Y, Yoshizawa T, Uchiyama Y, Yanagisawa M, Goto K, Masaki T, Kanazawa I (1989) Endothelin-3 is a novel neuropeptide: isolation and sequence determination of endothelin-1 and endothelin-3 in porcine brain. Biochem Biophys Res Comm 164:587–593

Skarphedinsson JO, Hårding H, Thorén P (1988) Repeated measurements of cerebral blood flow in rats. Comparisons between the hydrogen clearance method and Laser Doppler flowmetry. Acta Physiol Scand 134:133–142

Supattapone S, Simpson AW, Ashle CC (1989) Free calcium rise and mitogenesis in glial cells caused by endothelin. Biochem Biophys Res Comm 165:1115–1122

Symon L (1989) Calcium antagonists in brain ischemia- Experimental observations. In: Hartmann A, Kuschinsky W (eds) Cerebral ischemia and calcium. Springer, Berlin Heidelberg New York pp 131–138

Vigne P, Marsault P, Breittmayer P, Frelin C (1990) Endothelin stimulates phosphatidylinositol hydrolysis and DNA synthesis in brain capillary endothelial cells. Biochem J 266:415–420

Yanagisawa M, Kurihara H, Kimura S, Tomobe Y, Kobayashi M, Mitsui Y, Yazaki Y, Goto K, Masaki T (1988) Endothelin: a novel potent vasoconstrictor peptide produced by vascular endothelial cells. Nature 332:411–415

Yoshimoto S, Ishizaki Y, Kurihara H, Sasaki T, Yoshizumi M, Yanagisawa M, Yazaki Y, Masaki T, Takakura K, Murota S (1990) Cerebral microvessel endothelium is producing endothelin. Brain Res 508:283–285

Yoshishawa T, Shinmi O, Giaid A, Yanagisawa M, Gibson SJ, Kimura S, Uchiyama Y, Polak JM, Masaki T, Kanazawa I (1990) Endothelin: A novel peptide in the posterior pituitary system. Science 247:462–464

Zini I, Grimaldi R, Merlo Pich E, Zoli M, Fuxe K, Agnati LF (1990) Aspects of neural plasticity in the central nervous system-V. Studies on a model of transient forebrain ischemia in male Sprague-Dawley rats. Neurochem Int 16:451–468

Zoli M, Merlo Pich E, Cimino M, Lombardelli G, Peruzzi G, Fuxe K, Agnati LF, Cattabeni F (1990) Morphometrical and microdensitometrical studies on peptide- and tyrosine hydroxylase-like immunoreactivities in the forebrain of rats prenatally exposed to methylazoxymethanol acetate. Develop Brain Res 51:45–61